JOURNAL OF APPLIED ELECTROCHEMISTRY **27** (1997) 422–427

On the behaviour of tin-containing species in cryolite–alumina melts

J. -H. YANG*, J. THONSTAD

Department of Electrochemistry, Norwegian Institute of Technology, N-7034 Trondheim, Norway

Received 11 March 1996; revised 29 August 1996

Tin oxide (SnO_2) dissolves in cryolite–alumina melts forming tetravalent tin species, but under reducing conditions it is reduced to divalent tin and, further, to metallic tin. Freezing point depression data for SnF_2 and SnO in molten cryolite (Na_3AlF_6) corresponded to the formation of one and two new particles, respectively. By anodic dissolution of tin into cryolite-alumina melts divalent as well as tetravalent tin was formed, depending on current density and composition. During electrolysis of SnO_2-based oxygen-evolving anodes, the condensate above the melt contained both divalent (SnF_2) and tetravalent (SnO_2) tin species.

1. Introduction

Tin oxide (SnO_2) is an interesting semiconductor and functional material. SnO_2-based materials have been applied in many fields, such as gas sensors, electrode materials, electrodes for glass melting furnaces and In–Sn oxide conducting glass [1–3]. In the field of aluminium electrolysis, SnO_2 is a candidate material for oxygen-evolving, nonconsumable anodes, so-called inert anodes, as a replacement for the consumable carbon anodes used today.

Tin oxide has a certain solubility in cryolite melts. As shown by Xiao *et al.* [4], the solubility of tin oxide in $NaF–AlF_3–Al_2O_3$ melts varies within the range 0.05–0.007 wt% SnO_2, depending on the concentration of Al_2O_3, the NaF/AlF_3 ratio and the temperature. The dissolved species are most likely complexes of the type $SnO_2AlF_6^{3-}$, $SnOF_4^{2-}$ and $Sn_2O_2F_8^{4-}$ [4]. It was found that the solubility of SnO_2 increased with decreasing oxygen partial presssure over the melts, when the composition of the reducing atmosphere (CO_2/CO = 85/15 and 95/5) was adjusted so as to avoid the formation of metallic tin. The increased solubility beyond the solubility of tetravalent tin oxide was taken as an indication of the formation of divalent tin species in the melt.

Information about the behaviour of lower-valent species of tin in fluoride melts was not found in the literature, while it has been studied in chloride melts. Castrillejo *et al.* [5] investigated the stability of tin chloride in $ZnCl_2$–NaCl melts and observed a wide stablity range of $SnCl_2$. Elizarov and Novichkov [6] studied the behaviour of tin salts in NaCl–KCl melts. The concentration was found to decrease with time due to vaporization of $SnCl_2$ and $SnCl_4$. Voltammograms showed peaks corresponding to the redox pairs Sn/Sn^{2+} and Sn^{2+}/Sn^{4+}. It was found that $SnCl_2$ decomposed slowly into Sn and $SnCl_4$. Delimarskii and Zarubiskii [7] observed that during anodic dissolution of tin in a 75%$SnCl_2$–20%KCl–5%$ZnCl_2$ melt, the current efficiency with respect to divalent tin varied from 116 to 101% with increasing current density, which was taken as an indication of the co-formation of monovalent and divalent tin during anodic dissolution.

Information on different valencies of tin-containing species and their behaviour in cryolite melts will improve the understanding of the mechanism of corrosion of inert anodes caused by the dissolution of tin species into the electrolyte, the interaction between dissolved metal [8] and tin species, and the transfer of tin to the cathode metal and to the gas phase. The present work encompasses the detection of dissolved divalent tin species, cryoscopy of the $Na_3AlF_6–SnF_2$ and $Na_3AlF_6–SnO$ systems, studies of the anodic dissolution of tin in $Na_3AlF_6–Al_2O_3$ melts and the analysis of condensates of tin species.

2. Experimental details

2.1. *Chemicals*

Hand-picked natural Greenland cryolite with a melting point of 1011 °C was used. All other chemicals were of analytical grade and were used without further treatment. Stannous fluoride (99% SnF_2) and oxide (99.5% SnO) and 99.9% pure tin were used. The SnO_2-based anodes were provided by Metoxit (Switzerland) with the composition 97% SnO_2, 2% Sb_2O_3, 1% CuO.

2.2. *Test apparatus and procedures*

2.2.1. Cryoscopy. Thermal analysis was performed in a conventional vertical tube furnace under argon atmosphere. A description of the experimental ar-

* Permanent address: Department of Metallurgy, Central-South University of Technology, Changsha 410083, China.

rangement and some details can be found elsewhere [9, 10]. Supercooling of the melt was minimized by vigorous stirring, use of a slow cooling rate (0.7 °C min^{-1}), and frequent seeding with small cryolite crystals to the melt. The solutes SnF_2 and SnO were added through a separate sintered alumina tube after the cryolite was melted, in order to minimize possible losses due to the low boiling point (781 °C) of SnF_2 [11] and the reported instability of SnO above 300–400 °C [3, 12]. A nickel crucible, a nickel stirrer and a nickel sheath for the calibrated Pt–Pt 10% Rh thermocouple were used, since nickel should not influence the measurements, according to the following thermodynamic data:

$$Ni\,(s) + SnF_2\,(g) = Sn\,(1) + NiF_2\,(s) \qquad (1)$$

$$\Delta G^0_{1300\,K} = 43.796\ kJ\,mol^{-1}$$

$$Ni(s) + SnO\,(s) = Sn\,(1) + NiO\,(s) \qquad (2)$$

$$\Delta G^0_{1300\,K} = 32.630\ kJ\,mol^{-1}$$

2.2.2. Anodic dissolution of tin. A sketch of the apparatus is shown in Fig. 1. The Na_3AlF_6–Al_2O_3 (sat.) melt was contained in a crucible made of sintered alumina. A small boron nitride (BN) crucible was used as the container for the tin anode, a tungsten or molybdenum wire with a sintered alumina sheath providing the electrical contact to the tin. The results of blank experiments and ICP analysis (Inductively Coupled Plasma emission spectrometer) of the tin anode showed that the quantity of W or Mo dissolved into the liquid tin during the experiments was negligible (< 0.006%). A Mo wire (3 mm diam.) was used as cathode. The cell was contained in a conventional vertical tube furnace under argon atmosphere. A potentiostat (PAR model 173) supplied constant current for the anodic dissolution of tin; the electrolysis time was recorded by a stopwatch and the current density was calculated in terms of the current divided by the working area, that is, the difference in area between the cross section of the BN crucible and the cross section of the alumina sheath.

Each test was conducted in the following manner. The BN crucible containing about 4 g of tin was lowered into the melt and kept for approximately 20 min to equilibrate the temperature. The experimental temperature was 1010 ± 3 °C. Electrolysis was performed for 15 min to 1 h in order to pass the same amount of charge (~0.108 Ah) for different currents. After electrolysis the BN crucible with liquid tin and electrolyte was raised above the melt and kept there for 5–10 min to cool, before being taken out of the furnace. The electrolyte adhering to the tin was carefully removed mechanically and the tin was weighed. The anodic dissolution of tin was determined from the weight loss during the experiments. All tests were duplicated.

2.2.3. Volatility studies. The melt was contained in a sintered alumina crucible with a graphite lid or sintered alumina lid. When electrolysis was applied, the melt was contained in a graphite crucible with an alumina lining and a graphite lid, as shown in Fig. 2. To collect any volatile species an outlet tube (9) passed through the lid and all the way out of the closed furnace. The inlet gas to the furnace was argon, the exit gas passed through the outlet tube and a plastic tube connected to an absorption bottle containing a solution of 30% $AlCl_3{\cdot}6H_2O$ and dilute HCl. After the experiment the condensates inside the tubes were washed out and transfered into a volumetric flask together with the absorption solution and analysed for tin by ICP. Condensates were also collected for XRD (X-ray diffraction) analysis.

3. Results and discussion

3.1. *Preliminary tests on the detection of divalent tin*

A few tests were performed in sintered alumina crucibles at 1030 °C in a closed furnace with SnO_2

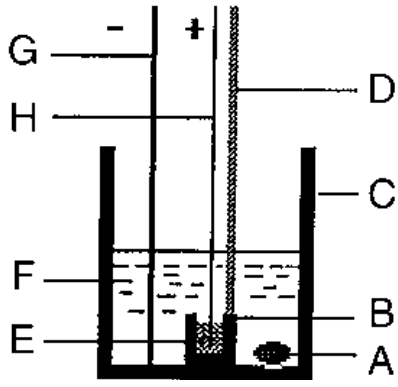

Fig. 1. Sketch of the experimental cell used for the study of anodic dissolution of tin. (A) metallic tin, (B) BN crucible (OD 16 mm, ID 8 mm and height 20 mm), (C) sintered alumina crucible, (D) Mo wire (2 mm) with sintered alumina sheath, (E) anode: metallic tin (~4 g), (F) electrolyte, (G) cathode: Mo wire (3 mm) and (H) W or Mo wire (1 mm) with a sintered alumina sheath (OD 3 mm).

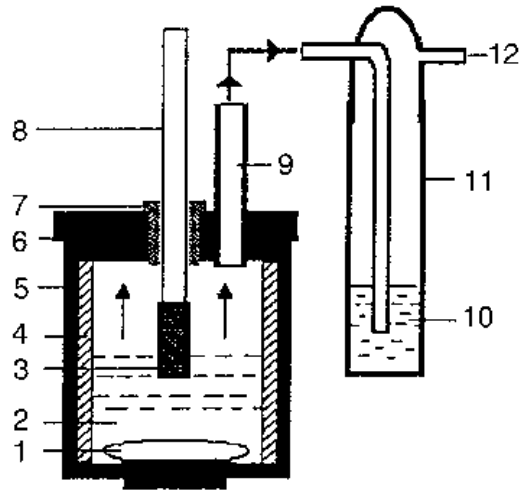

Fig. 2. The cell for volatity studies. (1) Molten aluminium, (2) electrolyte (~200 g), (3) SnO_2-based anode, (4) sintered alumina lining, (5) graphite crucible, (6) graphite lid, (7) boron nitride insulation, (8) steel holder for anode, (9) sintered alumina gas exit tube, (10) 30 wt % $AlCl_3 \cdot 6H_2O$ + dilute HCl solution, (11) wash bottle and (12) gas outlet.

powder added to saturated cryolite-alumina melts, and a CO_2/CO gas mixture of ratio 85/15 being flushed over the melt. The experimental details can be found in [4]. Samples of the melt were siphoned out after 5 h and 7 h. The samples were crushed and dissolved in a solution of 30% $AlCl_3{\cdot}6H_2O$ + dilute HCl at 80 °C (a $NaHCO_3$ solution was dripped continuously into the solution to generate CO_2 to prevent the oxidation of Sn^{2+}). A qualitative test using ammonium phosphomolybdate solution showed that divalent tin was present in the solution.

In another experiment, metallic aluminium, SnO_2 powder (contained in a smaller sized alumina crucible (ID: 25 mm × 25 mm) separate from the aluminium) and the same melt as above were contained in a sintered alumina crucible (ID: 58 mm × 108 mm) in argon atmosphere. The first sample of the melt was taken 0.5 h after the melt had reached 1010 °C. Qualitative analysis showed that divalent tin was present in the melt. But after two hours no divalent tin was traced in the melt, which indicates that in the presence of dissolved aluminium, SnO_2 is reduced to divalent tin dissolved in the melt and further to metallic tin.

3.2. *Cryoscopy of the systems Na_3AlF_6–SnF_2 and Na_3AlF_6–SnO*

Figure 3 shows freezing point depression data for the systems Na_3AlF_6–SnF_2 and Na_3AlF_6–SnO compared to calculated liquidus lines for the formation of various numbers of units (c) of foreign species by the addition of one unit of the tin compound. The calculation procedure is outlined in [13]. The experimental results indicate that the number of new entities formed at infinite dilution is close to 1.0 for SnF_2 and close to 2.0 for SnO. The slight deviations from the theoretical lines may be caused by evaporation of the tin species. These cryoscopic numbers show that the tin and oxygen atoms most probably form one new species each. The formation of oxygen-containing divalent tin species can be ruled out in the range of dilute solutions. There is no sign of dimerization of tin ions like that of iron ions in the system Na_3AlF_6–FeF_2 [10].

3.3. *On the anodic dissolution of tin*

Conceivable anodic dissolution reactions for tin are:

$$Sn = Sn^{+} + e^{-} \tag{3}$$

$$Sn = Sn^{2+} + 2e^{-} \tag{4}$$

$$Sn = Sn^{4+} + 4e^{-} \tag{5}$$

Reaction 5 can occur in two steps: Reaction 4 followed by

$$Sn^{2+} = Sn^{4+} + 2e^{-} \tag{6}$$

In the present analysis we cannot distinguish between these reaction paths which have the same net result, so the treatment is restricted to Reactions 3–5. During anodic dissolution of tin, two of these reactions may occur simultaneously. Assuming that no anodic reactions other than Reactions 3–5, and no side reactions take place, we can use Faraday's law to calculate the proportion of partial currents carried by the different valences of tin ions. The effective or average charge number (n_{av}) can be calculated from the equation

$$\frac{I}{n_{av}F}t = \frac{\Delta W}{M_{Sn}} \tag{7}$$

where I is the current, t is the time, M_{Sn} is the molar weight of tin, and ΔW is the weight loss of tin during anodic dissolution.

Rearranging, gives

$$n_{av} = \frac{ItM_{Sn}}{\Delta WF} = \frac{I}{m_{exp}F} \tag{8}$$

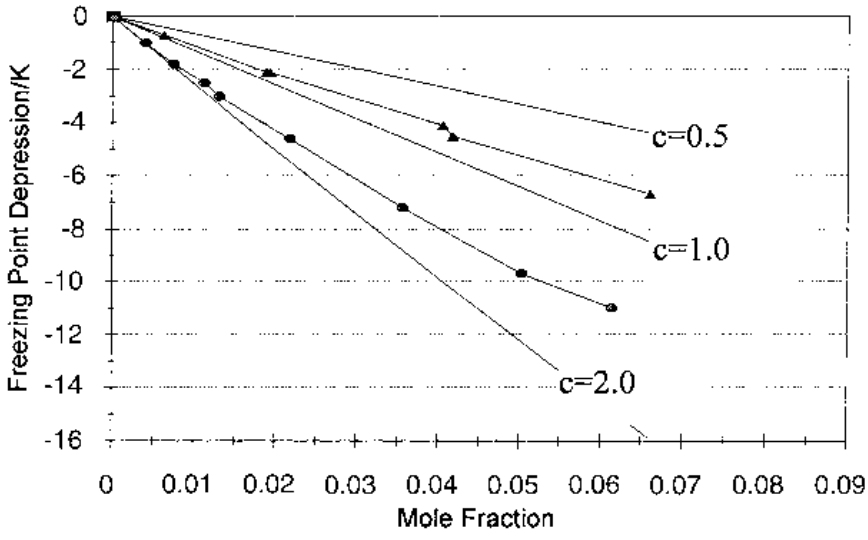

Fig. 3. Freezing point depression data for the systems Na_3AlF_6–SnF_2 and Na_3AlF_6–SnO compared to calculated liquidus lines for the formation of 0.5, 1 or 2 new entities by the addition of one unit of the tin compounds. (▲)SnF_2, (●)SnO.

Table 1. Correlation between n_{av}, the total current (I), the partial currents and the number of moles dissolved per second

n_{av}	I	$\frac{I}{n_{av}F}$	*Equations*
4	$I_{Sn(IV)}$	$\frac{I}{4F}$	
2 < n < 4	$I_{Sn(II)} + I_{Sn(IV)}$	$\frac{I_{Sn(II)}}{2F} + \frac{I_{Sn(IV)}}{4F}$	10
2	$I_{Sn(II)}$	$\frac{I}{2F}$	
1 < n < 2	$I_{Sn(I)} + I_{Sn(II)}$	$\frac{I_{Sn(I)}}{F} + \frac{I_{Sn(II)}}{2F}$	11
1	$I_{Sn(I)}$	$\frac{I}{F}$	

where m_{exp} is the number of moles of tin which dissolves anodically into the melt per unit time. Blank experiments without electrolysis showed that losses of tin were negligible (<0.003 g h^{-1}).
In general,

$$I = I_{Sn(I)} + I_{Sn(II)} + I_{Sn(IV)} \quad (9)$$

where $I_{Sn(I)}$, $I_{Sn(II)}$ and $I_{Sn(IV)}$ are the partial currents carried by Reactions 3, 4, 5, respectively, during anodic dissolution of tin. Five limiting cases are shown in Table 1.

Anodic dissolution tests were conducted in three different melts: Na_3AlF_6–Al_2O_3, Na_3AlF_6–Al_2O_3 (sat)–SnF_2 (2 wt %) and Na_3AlF_6–Al_2O_3 (sat)–SnO_2 (sat). Experimental data are given in Table 2. These show that $n_{av} \geq 2$ at all current densities in the melts investigated, which indicates that tin dissolves anodically as Sn^{2+} and Sn^{4+}. There was no evidence of formation of Sn^{+}. This result differs from that of Delimarskii and Zarubiskii [7] obtained in $SnCl_2$-rich chloride melts, as mentioned above.

The partial currents of Sn^{2+} and Sn^{4+} (in per cent) calculated from Equation 11 as a function of the anodic current density, are plotted in Fig. 4. This shows that the proportion of Sn^{2+} increases with increasing current density while that of Sn^{4+} decreases.

Table 2. Average charge number (n_{av}) for anodic dissolution of tin in the three melts (A: Na_3AlF_6–Al_2O_3 (sat); B: Na_3AlF_6–Al_2O_3 (sat)–SnF_2(2 wt %); C: Na_3AlF_6–Al_2O_3 (sat)–SnO_2(sat)) at various current densities

Current density /A cm^{-2}	*Average charge number (n_{av})* *Melt A*	*Melt B*	*Melt C*
0.1			2.73
0.2		4	2.59
0.3	2.66	4.05	2.69
0.6		3.35	
0.9		2.99	
1.2	2.32	2.37	2.37
1.5		2.27	
1.9	2.30		
2.1		2.30	
2.5	2.23		
2.6			2.27
2.9		2.16	

For the Na_3AlF_6–Al_2O_3 (sat)–SnF_2 (2 wt %) melt, practically only Sn^{4+} forms at current densities below 0.3 A cm^{-2}. A possible explanation of the experimental data is as follows. At high current densities, the limited solubility of Sn(IV) in saturated cryolite–alumina melts tends to inhibit the formation of Sn(IV), so that divalent tin is mainly formed. On the other hand, the presence of SnF_2 in the melt (in Na_3AlF_6–Al_2O_3(sat)–SnF_2 (2 wt %)) inhibits the formation of Sn(II) species. At low current densities, fast and reversible charge transfer of tin to form divalent tin (Equation 4), as verified by voltammetry [14], favours further formation of tetravalent tin.

3.4. *On the volatility of dissolved tin species*

As mentioned in Section 2.2.1, the boiling point of SnF_2 is low (781 °C), SnO is thermodynamically unstable above 300–400 °C while SnF_4 sublimates at 705 °C [15]. Hence, possible volatility of tin species in

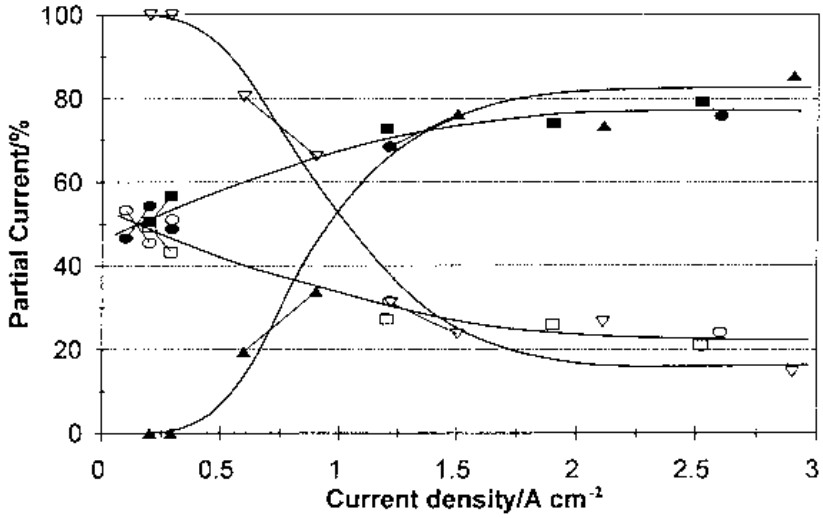

Fig. 4. The correlation between partial currents (in per cent) carried by Sn(II) and Sn (IV); and the current density during anodic dissolution of tin in the following melts: (A) Na_3AlF_6–Al_2O_3, (■) Sn(II), (□) Sn(IV); (B) Na_3AlF_6–Al_2O_3(sat)–SnF_2 (2 wt %), (▲) Sn(II), (▽) Sn(IV); (C) Na_3AlF_6–Al_2O_3(sat)–SnO_2(sat), (●) Sn(II), (○) Sn(IV).

Table 3. The content of tin in the vapour phase above cryolite–alumina (sat) melts containing tin species at 1010 °C

Melts Tin species	*Al*	*Time* /h	*Electrolysis*	*Sn amount in the vapour phase* /g
SnO_2	no	16	no	0.0002
SnO_2*	no	16	no	0.0253
2% SnF_2	no	16	no	0.219
SnO_2†	yes	16	no	0.0016
SnO_2 anode	yes	6.3	yes	0.0704

* A graphite lid was used.
† SnO_2 was located in a smaller sized alumina crucible, separate from the aluminium in melt.

the melts during electrolysis with SnO_2-based anodes is of interest.

Some simple experiments were run to look for tin species in the condensate above Na_3AlF_6–Al_2O_3(sat) melts contained in alumina crucibles under varying conditions, that is, by adding SnO_2 or SnF_2, with aluminium present and by running electrolysis. As shown in Table 3, over a pure Na_3AlF_6–Al_2O_3 (sat)–SnO_2 (sat) melt under argon only traces of tin were detected. When a graphite lid was used, a dramatic increase in volatility was observed, probably caused by traces of air forming CO ($2C + O_2 = 2CO$) and subsequently divalent tin. Addition of divalent tin in the form of 2% SnF_2 (no graphite present) gave rise to high volatility. The presence of aluminium and SnO_2 (kept in separate containers) and application of electrolysis also produced tin-containing condensate.

It must be stated that several factors (such as gas flow rate etc.) may influence the volatility. In this preliminary study the experimental conditions were not well controlled, so the values given are only qualitative and vapour pressure data cannot be derived.

The electrolysis current with SnO_2-based anodes was 3.6 A and the anodic current density was about 0.8 A cm^{-2}. To estimate the corrosion rate of the SnO_2 anode, the amounts of tin contained in the metal, in the cryolite melt and in the vapour phase were summed. Table 4 shows the distribution of tin corroded from the anode after electrolysis for 6.3 h. The amounts of tin were converted to SnO_2 and divided by the working anode surface area and the duration of electrolysis, yielding a corrosion rate of the anode of 0.019 g cm^{-2} h^{-1}. This is in fair agreement with the results of Xiao *et al.* [16].

The content in the electrolyte is far above saturation for tetravalent SnO_2 [4], indicating the presence of some divalent tin. During steady state electrolysis the content in the electrolyte remains constant, so that the corrosion products from the anode are distributed between the metal and the gas phase. The data in Table 4 implies that as much as 24% of the corrosion products may end up in the condensate. However, it should be noted that the ratio between the surface areas of cathode and anode was very unfavourable (~5) in this case, which may promote the formation of volatile divalent tin species.

Table 4. Distribution of corrosion products from the anode, counted as SnO_2, after electrolysis for 6.3 h

	Amount of SnO_2 / %	/g	Per cent of total / %
Electrolyte	0.075	0.15	28
Metal	0.96	0.30	55
Condensate	–	0.089	17

XRD analyses were performed on samples of condensate collected from the outlet tube of the cell after electrolysis under the same electrolysis conditions as in Table 3. On the XRD diagram shown in Fig. 5, SnF_2 and SnO_2 were detected together with NaF-AlF_3 compounds. The presence of SnF_4 (no ASTM card available) and SnO cannot be ruled out because there are unidentified peaks in the diagram.

The presence of SnF_2 suggests an interaction between the corrosion product (Sn(IV)) and dissolved metal to form divalent tin as indicated above. The SnO_2 in the condensate probably came from the oxidation of SnO(g) ($2\ SnO + O_2 = 2\ SnO_2$). Another possible source of SnO_2 was fine SnO_2 particles being detached from the anode and entrained in the anode gas. Furthermore, some SnF_4 may evaporate, due to the exchange reaction

$$SnO_2(diss) + 4/3AlF_3 = 2/3\,Al_2O_3 + SnF_4(g) \quad (12)$$

4. Conclusions

Tetravalent tin species dissolved in cryolite–alumina melts can be transformed to divalent tin or metallic tin under reducing conditions. The results indicate that there is an interaction between dissolved aluminium in the melt and tetravalent tin to form divalent tin which can evaporate or be further reduced to metallic tin. The results for anodic dissolution of tin demonstrated the coformation of divalent and tetravalent tin in cryolite–alumina melts.

Acknowledgement

Financial support from the Norwegian Research Council and from the Norwegian aluminium industry is gratefully acknowledged. Thanks are due to T. Tharaldsen for XRD analysis and also to T. Eggen, L. I. Støen, E. Gudbransen, E. Olsen and H. Skybakmoen for their assistance.

References

[1] S. J. Blunden, P. A. Cusack and R. Hill, 'The Industrial Uses of Tin Chemicals', The Royal Society of Chemistry, London (1985).
[2] J. F. McAleer, P. T. Moseley, J. O. Norris, W. D. E. Williams, P. Taylor and B. C. Tofield, *Mater. Chem. Phys.* **17** (1987) 577.

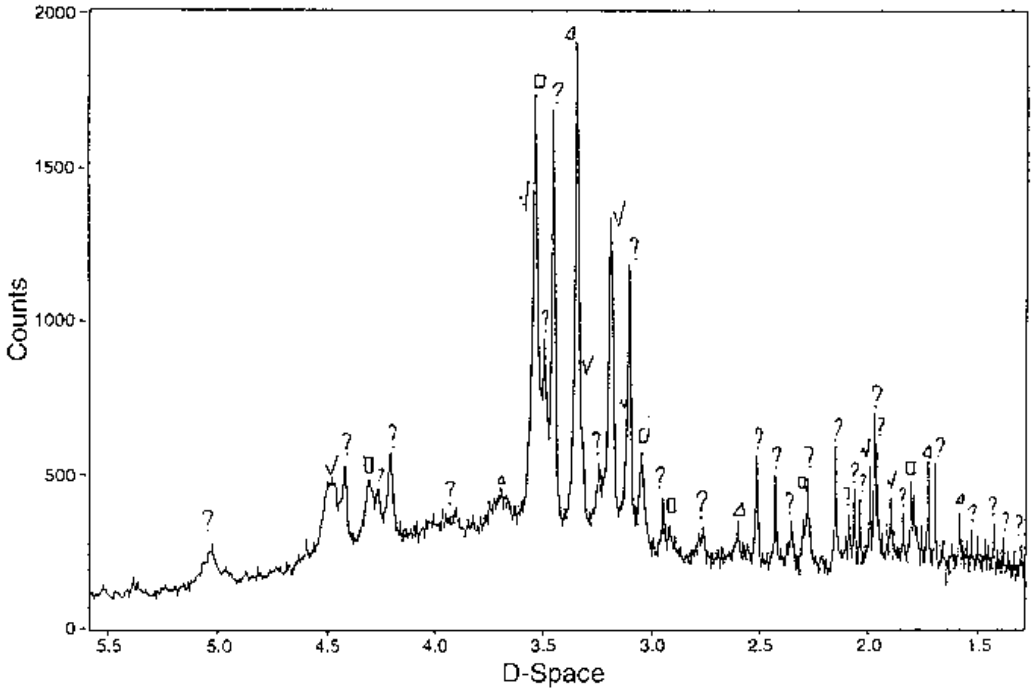

Fig. 5. X-ray diffraction diagram for analysis of the condensate after electrolysis of a SnO_2-based anode in Na_3AlF_6–Al_2O_3 (sat) melt. Legend: (√) SnF_2; (△) SnO_2; (□) $NaAlF_4$; (?) SnF_4; (?) SnO.

[3] L. -Z. Yang, Z. -T. Sui and C. -Z. Wang, *J. Solid State Chem.* **113** (1994) 221.
[4] H. Xiao, J. Thonstad and S. Rolseth, *Acta Chem. Scand.* **49** (1995) 96.
[5] Y. Castrillejo, D. Ferry, A. Garcia, R. Pardo and P. Sanchez Batanero, *Mater. Sci. Forum*, **73–75** (1991) 341.
[6] D. V. Elizarov and V. Y. Novichkov, *Rasplavy* **4** (1992) 93.
[7] I. K. Delimarski and O. G. Zarubitski, *Metallurgia*, Moscow (in Russian), (1975) 74.
[8] K. Grjotheim, C. Krohn, M. Malinovsky, K. Matiasovsky and J. Thonstad, 'Aluminium Electrolysis,' 2nd ed., Aluminium Verlag, Duesseldorf (1982).
[9] A. Solheim, S. Rolseth, E. Skybakmoen and L. Støen, 'Light Metals 1995' (edited by J. Evans), TMS, Warrendale, PA (1995) p. 451.
[10] H. G. Johansen, Å. Sterten and J. Thonstad, *Acta Chem. Scand.* **43** (1989) 417.
[11] O. Knacke, O. Kubaschewski, K. Hesselmann (eds.), 'Thermodynamic Properties of Inorganic Substances,' 2nd edn, Part 2, Springer-Verlag, Berlin (1991).
[12] L. V. Gurvich, I. V. Veyts and C. B. Alcock (eds) 'Thermodynamical Properties of Individual Substances', 4th edn, vol.2, part.1, Hemisphere, New York (1991) p. 356.
[13] Å. Sterten and I. Mæland, *Acta Chem. Scand.* **39** (1985) 241.
[14] L. Issaeva, J. -H. Yang, G. M. Haarberg, J. Thonstad and N. Alberg, *Electrochim. Acta*, to be published.
[15] R. C. Weast, D. R. Lide, M. J. Astle and W. H. Beyer (eds.) *in* 'CRC Handbook of Chemistry and Physics', 70th edn, CRC Press (1989–1990) p. B-139.
[16] H. Xiao, R. Hovland, S. Rolseth and J. Thonstad, 'Light Metals 1992' (edited by E. R. Cutshall), TMS, Warrendale, PA (1992) p. 389.